Article

Design, Synthesis and Properties of a Potent Inhibitor of *Pseudomonas aeruginosa* Deacetylase LpxC

Grazia Piizzi, David T. Parker, Yunshan Peng, Markus Rolf Dobler, Anup Patnaik, Som Wattanasin, Eugene Liu, Francois Lenoir, Jill Nunez, John Kerrigan, David McKenney, Colin S. Osborne, Donghui Yu, Leanne Lanieri, Jade Bojkovic, JoAnne Dzink-Fox, Maria-Dawn Lilly, Elizabeth R. Sprague, Yipin Lu, Hongming Wang, Srijan Ranjitkar, Bing Wang, Meir Glick, Lawrence G. Hamann, Ruben Tommasi, Xia Yang, and Charles R. Dean

Just Accepted

1
2
3
4
5
6
7
8
9
10
11
12
13
14
15
16
17
18
19
20
21
22
23
24
25
26
27
28
29
30
31
32
33
34
35
36
37
38
39
40
41
42
43
44
45
46
47
48
49
50
51
52
53
54
55
56
57
58
59
60

Discovery Chemistry

Ranjitkar, Srijan; Novartis Institutes for BioMedical Research Emeryville, Infectious Diseases

Wang, Bing; Novartis Institutes for BioMedical Research, Global Discovery Chemistry

Glick, Meir; Novartis Institutes for BioMedical Research, Global Discovery Chemistry

Hamann, Lawrence; Novartis Institutes for BioMedical Research, Global Discovery Chemistry

Tommasi, Ruben; Novartis Institutes for BioMedical Research, Global Discovery Chemistry

Yang, Xia; Novartis Institutes for BioMedical Research Emeryville, Infectious Diseases

Dean, Charles R. ; Novartis Institutes for BioMedical Research Emeryville,

SCHOLARONE™
Manuscripts

Design, Synthesis and Properties of a Potent Inhibitor of *Pseudomonas aeruginosa* Deacetylase LpxC

Grazia Piizzi*[1], David T. Parker[1], Yunshan Peng[1], Markus Dobler[1], Anup Patnaik[1], Som Wattanasin[1], Eugene Liu[1], Francois Lenoir[1], Jill Nunez[1], John Kerrigan[1], David McKenney[2], Colin Osborne[2], Donghui Yu[2],Leanne Lanieri[2], Jade Bojkovic[2], JoAnn Dzink-Fox[2], Maria-Dawn Lilly[2], Elizabeth R. Sprague[3], Yipin Lu[1], Hongming Wang[1], Srijan Ranjitkar[2], Bing Wang[1], Meir Glick[4], Lawrence G. Hamann[1], Ruben Tommasi[1], Xia Yang[2] and Charles R. Dean*[2].

Global Discovery Chemistry[1], Infectious Diseases Area[2], Chemical Biology and Therapeutics[3], Lead discovery Informatics[4], Novartis Institutes for BioMedical Research, Cambridge MA, 02139[1,3,4] and Emeryville CA, 94608[2]

ABSTRACT

Over the past several decades the frequency of antibacterial resistance in hospitals, including multi-drug resistance (MDR) and its association with serious infectious diseases, has increased at alarming rates. *Pseudomonas aeruginosa* is a leading cause of nosocomial infections, and resistance to virtually all approved antibacterial agents is emerging in this pathogen. To address the need for new agents to treat MDR *P. aeruginosa*, we focused on inhibiting the first committed step in the biosynthesis of lipid A, the deacetylation of uridyldiphospho-3-*O*-(*R*-hydroxydecanoyl)-*N*-acetylglucosamine by the enzyme LpxC. We approached this through the design, synthesis and biological evaluation of novel hydroxamic acid LpxC inhibitors, exemplified by **1**, where cytotoxicity against mammalian cell lines was reduced, solubility and plasma-protein binding (PPB) was improved while retaining potent anti-pseudomonal activity *in vitro* and *in vivo*.

INTRODUCTION

Antibiotic resistance has become very widespread, threatening our continued ability to treat serious life threatening infections[1]. This issue is exacerbated in Gram-negative pathogens, as these bacteria are defined by the presence of an additional protective outer membrane (OM)[2]. The OM is an asymmetrical bilayer with a phospholipid inner leaflet and an outer leaflet comprised primarily of cross-linked lipopolysaccharide (LPS)[3]. The unique OM architecture provides an extra permeability barrier that protects the cells from toxic compounds and is important for bacterial survival during infection. The OM can limit compound influx, and this together with active efflux can prevent many antibacterial compounds from accumulating sufficiently within the cell to fully inhibit their targets[4, 5]. Many clinically used antibiotics that are effective against Gram-positive bacteria (which lack an OM), are ineffective against Gram-negative pathogens. The combination of the OM and efflux exacerbates the development of resistance to the limited armamentarium of Gram-negative agents. The OM also impacts efforts to discover and optimize new antibacterial scaffolds to achieve potent cellular activity against Gram-negative pathogens. Along with its role in forming the OM, LPS is essential for growth in many important Gram-negative pathogens, including *Escherichia coli*, *Klebsiella pneumoniae* and *P. aeruginosa*. LPS is not essential for *in vitro* growth in certain Gram-negative bacteria such as some *A. baumannii*[6], however, inhibition of lipid A biosynthesis may still be efficacious in treating infections by these organisms[7], and would be expected to increase susceptibility to other antibiotics by disrupting the OM permeability barrier[8]. For these reasons, lipid A biosynthesis[9, 10] and OM assembly[11] have been a major focus in antibacterial drug discovery.

LPS consists of a lipid anchor, lipid-A, which forms the outer leaflet of the OM, to which is attached a core oligosaccharide and a repeating carbohydrate O-antigen extending out from the

cell surface[3]. The first committed step of lipid A biosynthesis is mediated by the zinc metallo

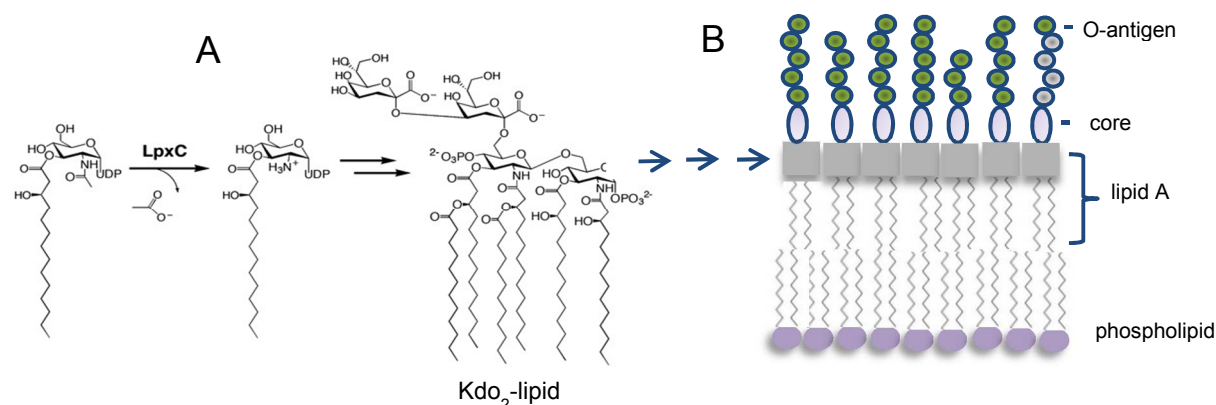enzyme LpxC (UDP-3-O-(acyl)-N-acetylglucosamine deacylase (Figure 1).

Figure 1. LpxC catalyzes the first irreversible step of lipid A biosynthesis in Gram-negative

bacteria (A). Multiple downstream steps complete the biosynthesis of lipid A which is then

linked to a core oligosaccharide and flipped across the inner membrane where it is then linked to

O-antigen oligosaccharide repeating units and transported out to form the outer leaflet of the

asymmetrical outer membrane (B).

LpxC is essential for growth of many Gram-negative pathogens, including *P. aeruginosa*[12] and

several groups designed potent inhibitors of LpxC enzymes[13-29]. However, despite extensive

medchem campaigns over the last decade (Figure 2), few inhibitors have reached the clinic and

no LpxC inhibitor has reached the market, underscoring the challenges to find a safe and

efficacious treatment for *P.a.* infections. One of the main challenges is to balance desirable

physicochemical properties, such as low PPB and high solubility, with potent antibacterial
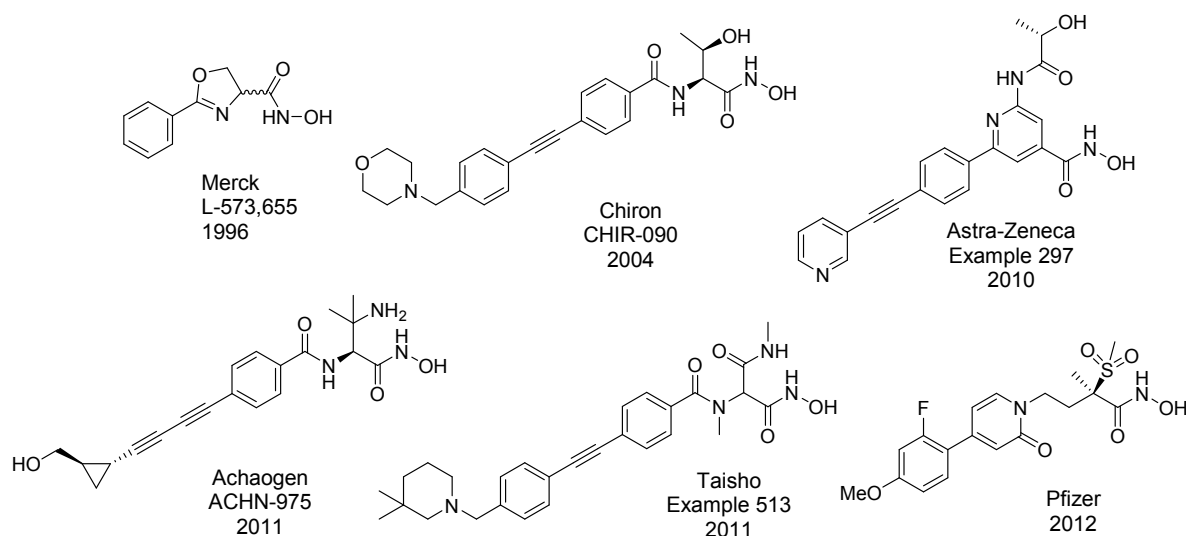
activity and low cytotoxicity[16].

Figure 2. Representative LpxC inhibitors resulting from drug discovery efforts over the last two decades. Compound **31** (CHIR-090) is described in Anderson et al[31], L-573,655 is described in Onishi et al[10] and ACHN-975 is described in Kasar et al[30].

RESULTS

Our efforts towards the discovery of potent and safe LpxC inhibitors began with the selection of a promising lead from Chiron's efforts in the early 2000's, hydroxamate **2**[31]. Similarly to **31**[26, 31, 32] (Figure 2), compound **2** has a zinc binding hydroxamate warhead with a hydrophobic tail that occupies the hydrophobic tunnel in the LpxC enzyme where the natural substrate fatty acid resides (Figure 3). While endowed with strong LpxC and antibacterial activity, compound **2** presented low aqueous solubility and undesireable *in vitro* cytotoxicity (Table 1). Thus, we initiated a structure-based design to identify modifications aimed at tackling both of these liabilities. A docking model of the binding of hydroxamate **2** revealed the proximity of the β-amino group to the UDP pocket of LpxC active site (Figure 3). Given that this large, solvent-exposed pocket is mostly unoccupied and possesses hydrophilic residues (e.g. Asp 196, Lys238 and Lys261) as well as backbone polar atoms, we targeted this region for further ligand interaction with the addition of water-solubilizing groups onto hydroxamate **2**.

Figure 3. Docking model of **2** bound to *P.a.* LpxC. LpxC is represented as a surface with polar residues colored (nitrogen is blue and oxygen is red). Compound **2** is shown in green sticks. The catalytic zinc is represented by a green sphere with dashes showing coordination by protein and **2**. Residues in the UDP pocket are labelled.
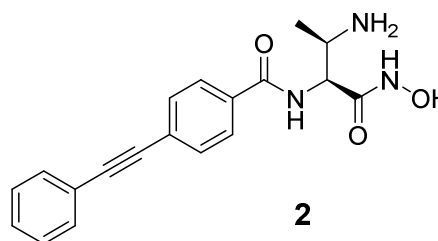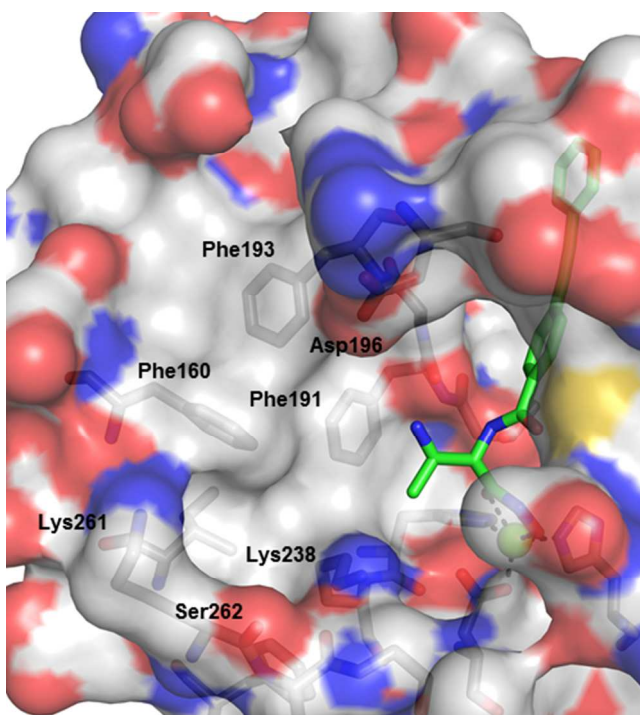
We started by screening several water-solubilizing groups that could occupy the UDP pocket. Our initial effort lead to analog **3** which retained excellent enzymatic potency, displayed greater aqueous solubility and lacked *in vitro* cytotoxicity (Table 1). Unfortunately, antimicrobial activity against wild-type *P.a.* (PAO1) was 32 fold weaker than analog **1** (MIC = 32 µg/mL vs 1 µg/mL, Table 1). However, *P.a.* defective for efflux (indicated as MIC Pump in Table 1), or having mutations leading to increased OM permeability (indicated as MIC Perm in Table 1) were susceptible to both analogs **2** and **3,** reflecting the retention of potent activity against the LpxC

1
2
3
4
5
6
7
8
9
10
11
12
13
14
15

target. These results suggested that analog **3** did not accumulate sufficiently in wild type cells to exert potent antibacterial activity.

Table 1. Initial attempt to add hydrophilic group on **2** expanding into UDP pocket*.
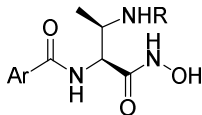
Compound	Ar	R	P.a. LpxC IC$_{50}$ (µg/mL)	MIC WT (µg/mL)	MIC Pump (µg/mL)	MIC Perm (µg/mL)
[a]**2**	1,2-diphenylethyne	H	0.0012	1	0.25	0.25
[b]**3**	1,2-diphenylethyne		0.002	32	0.5	4
4	4-ethyl-1,1'-biphenyl	H	0.0005	2	0.06	0.25
5	4-ethyl-1,1'-biphenyl		0.0004	128	1	32
6	4-ethyl-1,1'-biphenyl		0.002	16	0.125	1
7	4-ethyl-1,1'-biphenyl		0.041	128	2	16

[a]Compound **2**: HT-Sol pH 6.8 = 0.009 µM, Cytotoxicity K562 EC$_{50}$ = 29.5 µM; [b]Compound **3**: HT-Sol pH 6.8 = 0.392 µM, Cytotoxicity K562 EC$_{50}$ > 100 µM. WT is wild type P. aeruginosa PAO1 strain K767[33], the efflux deficient (Pump) strain is a K767 derivative deleted for *mexAB-oprM* (K1119)[34]. The drug hypersusceptible (Perm) strain is strain Z61[35].

Encouraged by these preliminary results on solubility and cytotoxicity, we decided to prepare additional analogs with substitution on the β-amino group in order to improve compound accumulation in wild type *P.a.*. We decided to replace the biphenyl acetylene tail of compound **2** and **3** with the biphenylethyl due to concerns over chemical and metabolic stability of the conjugated alkyne. Compounds **4-7** (Table 1) summarize the *in vitro* activity of the UDP series. Although excellent enzymatic potency similar to compound **3** was retained, we did not observe the expected improvement in antimicrobial activity. Indeed, the added polar groups had a negative impact on efflux properties and/or passive cell permeability (compounds **5-7** versus **4**). These compounds were prepared according to Scheme 1 starting with β-amino ester **8**[31]. Acylation or reductive amination of **8** allowed for the installment of the desired functionalities onto the β-amino group and furnished compounds **9a-9d**. Conversion of the resulting esters **9a-9d** to the corresponding hydroxamic acids **3**, **5-7** was carried out by standard conditions.

Scheme 1. Synthesis of key compounds for UDP pocket exploration.[a]

Ar =

R =

9a, 3

9b, 5

9c, 6

9d, 7

8

9a-9d

3, 5-7
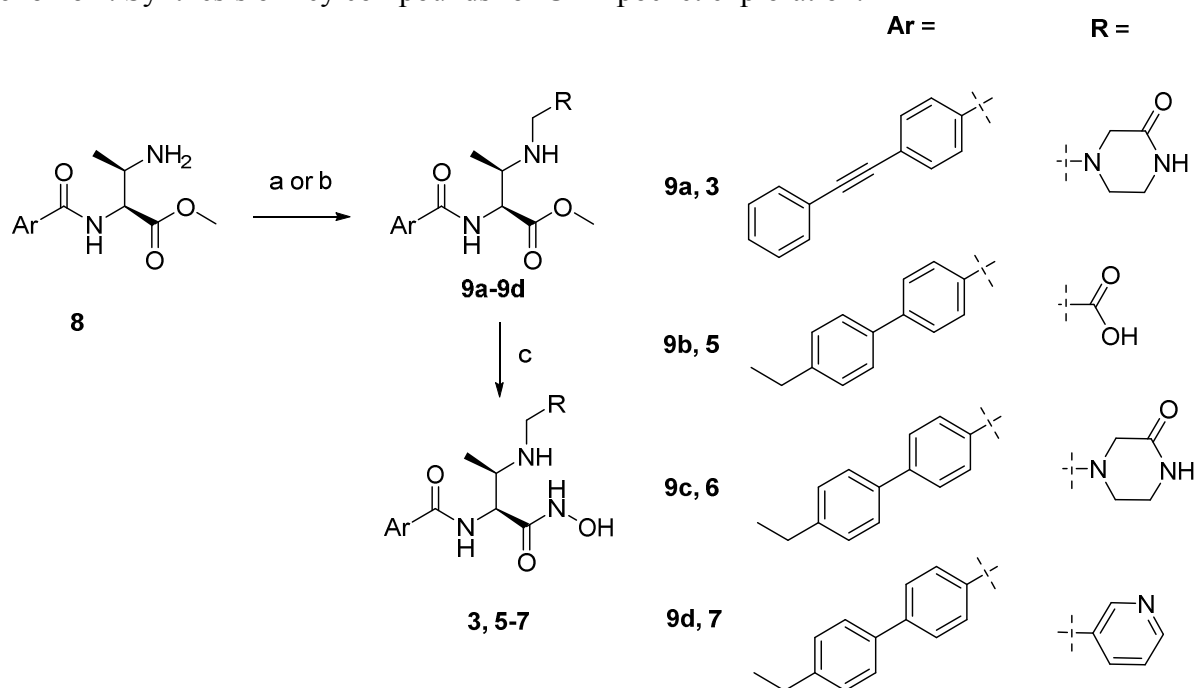
[a]Reagents and conditions: (a) Alkyl chloride, DMF, 50 °C, 36 h (**Compounds 3, 5, 6**); (b) 3-pyridine

carboxaldehyde, Sodium triacetoxyborohydride, DCE:DCM (2:1), rt, 16 h (**Compound 7**); (c) NH$_2$OH(aq) (50%

by wt), rt, 2 days.

We then turned our attention to the group occupying the hydrophobic tunnel of the enzyme

active site. We questioned whether the extended linear and conjugated biphenylethyl tail could

be shortened to reduce its hydrophobicity and improve physicochemical properties.

Representative examples from this exploration are summarized in Table 3[36]. Interestingly,

compound **10** with a replacement of the aromatic ring by a substituted cyclohexyl group retained

good target potency but had no appreciable antimicrobial activity in wt *P.a.*. Conformationally

constrained substituents on one aromatic ring (compounds **11-13**) yielded weak activity, mostly

due to compromised target potency. Extending the aromatic ring with a flexible hydrocarbon tail

restored enzymatic potency (compound **14**) but a propargyl tail, as in compound **15**, proved to be

the best fit, as of geometry and polarity, for the hydrophobic tunnel.

8

Table 2. Exploration of novel tails for the hydrophobic tunnel.
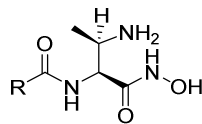
Compound	R	P.a. LpxC IC$_{50}$ (µM)	MIC WT (µg/mL)	MIC Pump (µg/mL)	MIC Perm (µg/mL)
10		0.035	128	16	32
11		0.53	>128	16	32
12		0.12	>128	>128	>128
13		0.083	32	1	4
14		0.011	8	0.5	1
15		0.006	2	0.25	0.5

Based on this initial propargyl tail result, we then explored whether the size or electronic properties of the substituent in β relative to the primary amino group could provide additional gains in potency. Compounds in Table 3 were prepared according to the procedures described[36]. A scalable synthesis of racemic and enantioselective **1 (+/-)** was disclosed in a recent publication [37]**.** Enantioselective synthesis of compound **20** is noteworthy and described in Scheme 2. Condensation of trifluoro acetal with *(S)-(-)-tert*-butanesulfinamide followed by diastereoselective addition of ethyl-2- ((diphenylmethylene)amino)acetate provided the desired chiral intermediate **17** in relatively low yield owing to instability of imine **16**. Cleavage of the

chiral auxiliary and protective group provided the diamino ester **18**. Selective acylation and

treatment with hydroxylamine yielded the final compound **20**.

Scheme 2. Synthesis of Compound **20**[a]
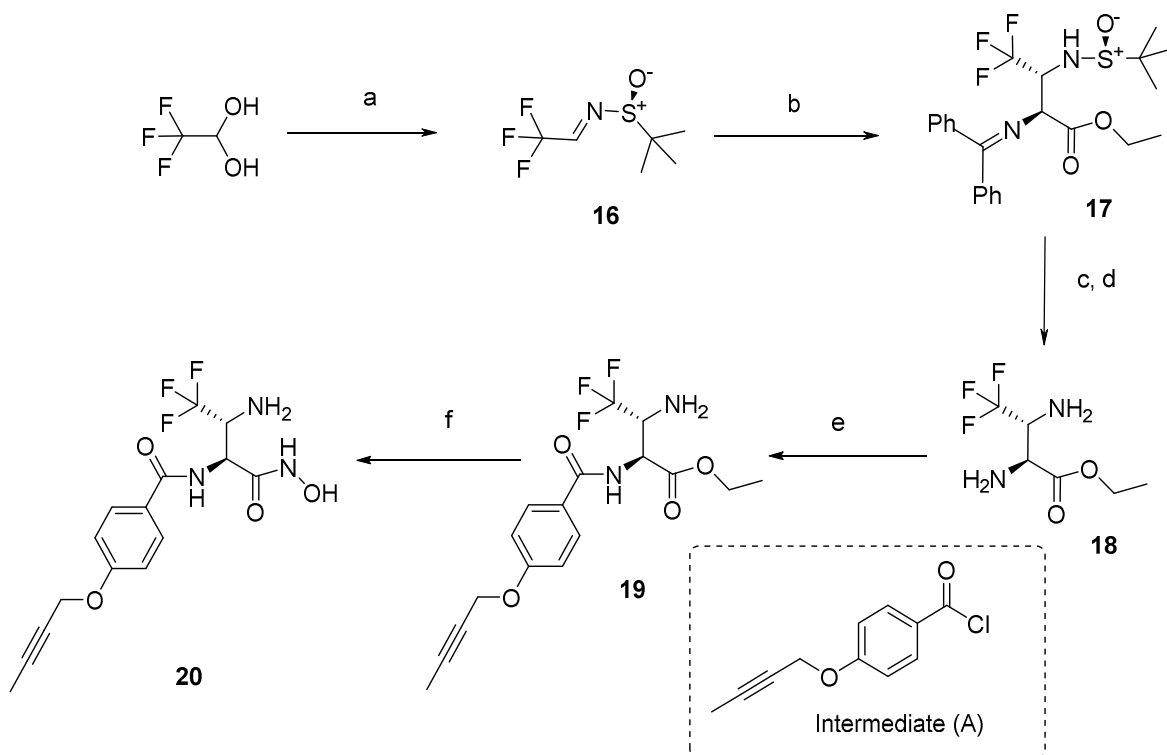
[a]Reagents and conditions: (a) Ti(OEt)$_4$, (S)-2-methylpropane-2-sulfinamide, Molecular sieves 4 A^0, DCM,

Reflux, 8 h; (b) LHMDS, Ethyl-2- ((diphenylmethylene)amino)acetate, THF, -78 ^{0}C to rt, 36 h, 17% (2 steps); (c)

Anhydrous HCl in EtOH (d) 2M HCl(aq), 100% (2 steps); (e) Intermediate (A), NaHCO$_3$(aq), 33%; (f)

NH$_2$OH(aq), MeOH:MeCN, 28%.

Addition of an extra methyl group in the β position of compound **15** was well tolerated even

when considering the activity of racemic compound **1** (Table 3). However, replacement of the

methyl group with larger and/or electron withdrawing substituents lead to weaker target and

cellular potency (**20-22**).

10

Table 3. SAR of the central core.
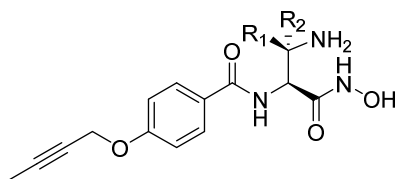
Compound	R_1	R_2	P.a. LpxC IC$_{50}$ (μM)	MIC WT (μg/mL)	MIC Pump (μg/mL)	MIC Perm (μg/mL)
1(+/-)	Me	Me	0.004	2	0.25	0.25
15	Me	H	0.006	2	0.25	0.5
20	H	CF3	0.014	16	0.25	1
21	i-pr	H	0.3	>128	16	32
22	(cyclopropyl)	H	0.12	32	2	4

To complete our SAR assessment of the propargyl ether series, we looked at the effect of the stereochemistry at the β position (monomethyl series) and that of the α position (gem-dimethyl series). Compound **15**, and single enantiomers **1-(-)** and **1-(+)** in Table 4 were prepared according to the procedure referenced above[36]. Single stereoisomer **30** was synthesized as described in Scheme 3. The synthesis began with trityl protection of methyl L-allothreoninate

11

followed by conversion of the alcohol **23** to azide **24** with inversion of stereochemistry under

Mitsunobu conditions. Trityl group of **24** was deprotected under acidic condition to furnish the

amine **25**, which was subsequently coupled to propargyl benzoic acid **26** using standard

amidation protocol to afford the amide **28** in good yield. Unlike the previously reported azide

reduction with PPh$_3$[31] that proved to be challenging in terms of purification, a smooth one pot

azide reduction of **27** with SnCl$_2$ followed by Boc-protection to **28** was accomplished. After

purification, **28** was deprotected to the corresponding amine **29** and the desired hydroxamic acid

30 was obtained by treatment of this ester with 50% NH$_2$OH(aq) at room temperature.
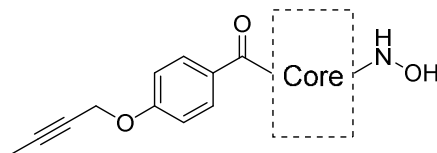
Scheme 3. Synthesis of Compound **30**[a].
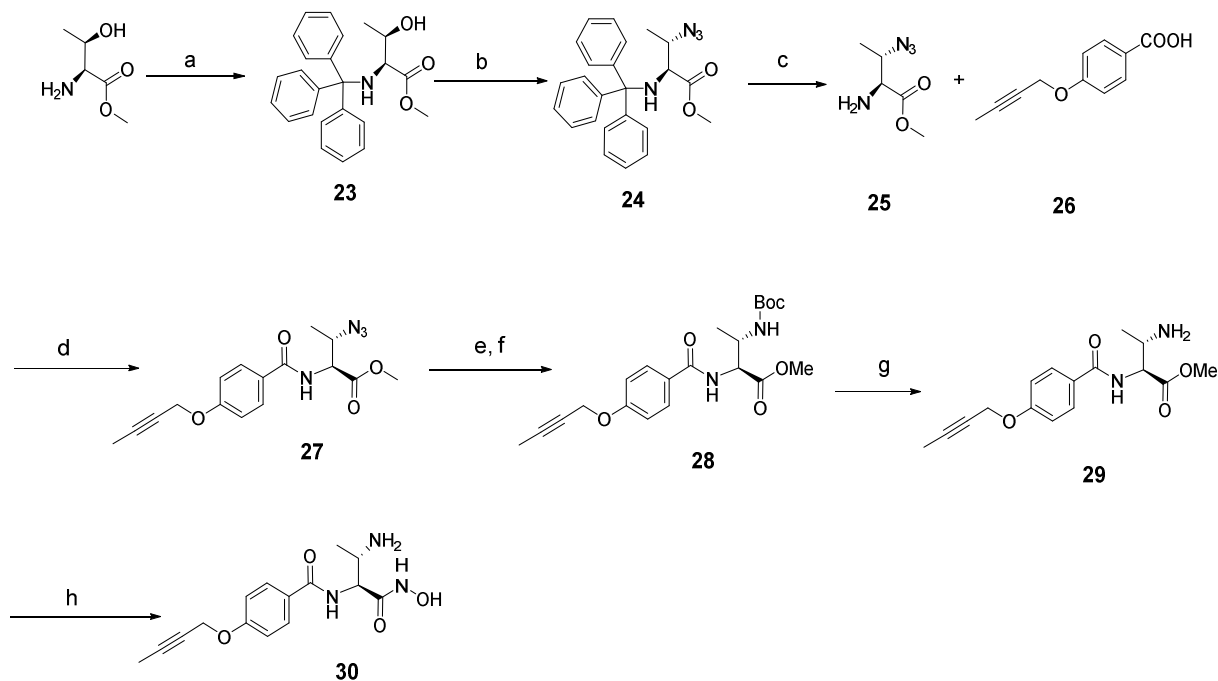
[a]Reagents and conditions: (a) TrCl, TEA, DCM, 0 °C – rt, quantitative yield; (b) DPPA, DIAD, PPh$_3$, THF, rt, 63%
(c) HCl, THF, rt, 85%; (d) HATU, DIPEA, DCM, rt, 51%; (e) SnCl$_2$, MeOH, rt; (f) (Boc)$_2$O, NaHCO$_3$, DCM, rt;
83% (2 steps); (g) TFA, DCM, rt; (h) NH$_2$OH (aq. 50%), MeOH, rt, 82 (2 steps).

The activity of the isolated stereoisomers is summarized in Table 4. While the β position was not sensitive to changes in stereochemistry (**15** and **30**), the α position of the gem-dimethyl series showed a clear preference for target inhibition and resulted in greater cellular potency for **1-(-)**.

Table 4. Effect of stereochemistry on enzymatic and antibacterial potency.

Compound	Core	P.a. LpxC IC$_{50}$ (μM)	MIC WT (μg/mL)	MIC Pump (μg/mL)	MIC Perm (μg/mL)
15		0.006	2	0.25	0.5
30		0.005	1	0.5	1
1(-)		0.001	0.5	0.06	0.25
1(+)		0.026	16	2	4

To gain further insight into the SAR of our inhibitors, we solved the co-crystal structure of *P.a.* LpxC with stereoisomer **1(-)**. We confirmed that the gem-dimethyl group in the β position was well accommodated adjacent to the UDP pocket. Likewise, the propargyl ether tail fits nicely in the hydrophobic tunnel, and the hydroxymate warhead retains optimal zinc coordination (Figure 4). Substitution of the phenyl acetylene with the propargyl ether reduced the mass and surface
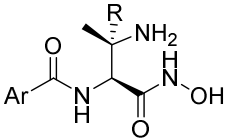
13

area of the compound yet maintains *in vitro* potency (similar target potency for compounds **15** and **1** versus compound **2**). Comparing the *P.a.* LpxC complex crystal structures with compounds having different tunnel binding groups (e.g. **31** vs compound **1**) suggests that the tunnel adapts to various tail groups via movement of the "gatekeeper" helix and neighboring residues (aa 192-205). Specifically, the movement of this helix repositions Ile197 in the upper part of tunnel to contribute a key nonpolar interaction with the propargyl tail (Figure 4). Additionally, the position of the primary amine allows for strong water network linking the $NH3^+$ group of the ligand to the protein via optimum hydrogen bonding with waters.

14
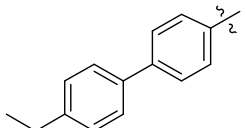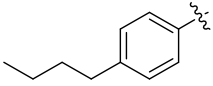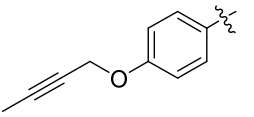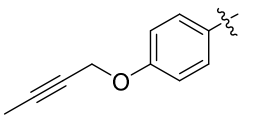
Figure 4. Co-crystal structure of *P.a.* LpxC with stereoisomer **1(-).** View of the hydrophobic tunnel enclosing the inhibitor. The protein surface is shown within 5Å of the compound and sidechains lining the tunnel are shown as sticks and labelled. Compound **1** is shown in green sticks. The catalytic zinc is represented by a green sphere.
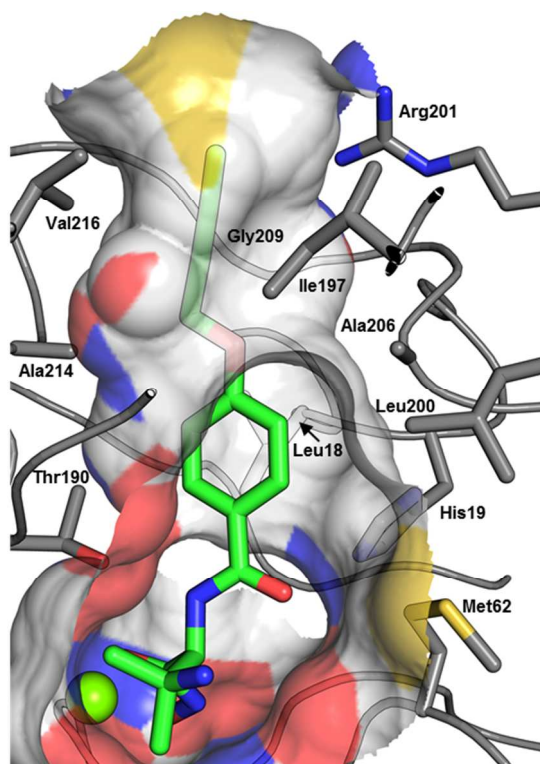
With this promising lead (compound **1(-)**) we next evaluated *in vitro* cytotoxicity and increased aqueous solubility. These were the two key liabilities of our starting point (compound **2**) we aimed to improve on (Table 1), and for the propargyl ether tail analogs (**15** and **1**) both liabilities had been addressed (Table 5).

Table 5. Cytotoxicity and solubility of selected analogs.

Compound	Ar	K562 IC$_{50}$ (μM)	HepG2 IC$_{50}$ (μM)	HT-Sol pH 6.8 (g/L)
4	(R = H)	7.37	12.78	0.004
14	(R = H)	42.3	125	>0.293
15	(R = H)	>419	>419	0.295
1(-)	(R = Me)	>295	>295	>0.327

Due to the presence of a strong zinc-binding warhead, we determined whether our potential lead candidate (compound **1 (-)**) was devoid of off-target activity including known metalloproteases. We confirmed strong selectivity of binding to LpxC (hHDAC 1-13 IC$_{50}$ > 30 uM, hMMPs IC$_{50}$ > 30 uM). Finally, the mouse, rat and human plasma protein binding (PPB) for compound **1**(-) determined using standard assays was 22.8, 22.1 and 80.7 % which was improved over that of the starting compound **2** (91.4, 92.8 and 91.9 %). Based on potency, solubility and clean *in vitro* cytotoxicity and selectivity profile, we selected **1 (-)** for further *in vitro* microbiology and *in vivo*

characterization. MIC values were determined for a small test panel of Gram-negative pathogens

and this indicated that potent antibacterial activity of **1 (-)** is limited primarily to *P. aeruginosa*

(Table 6).

Table 6. Susceptibility of various Gram-negative bacteria to compound **1(-).**

		MIC (µg/mL)	
Name	Strain #	**1 (-)**	Ciprofloxacin
Pseudomonas aeruginosa	NB52001	1	0.5
Pseudomonas aeruginosa	NB52096	2	2
Acinetobacter baumannii	NB48015	>128	0.5
Alcaligenes xylosus	NB56002	16	2
Burkholderia cepacia	NB49016	32	0.5
Stenotrophomonas maltophilia	NB55011	32	0.5
Enterobacter aerogenes	NB24004	>128	> 16
Escherichia coli	NB27047	64	≤ 0.03
Klebsiella pneumoniae	NB29018	16	≤ 0.03
Klebsiella oxytoca	NB30007	16	≤ 0.03
Proteus mirabilis	NB32022	64	≤ 0.03

We then measured the antimicrobial activity of **1 (-)** and comparator antibiotics against a broad

panel of 180 *P. aeruginosa* clinical isolates from the Novartis strain collection and this is

summarized in Table 7. This panel included 96 isolates that were resistant to multiple standard

antibiotics according to CLSI breakpoints. The MIC_{50} and MIC_{90} values against this panel were

1 µg/mL and 2 µg/mL, respectively, with a range of MIC values of ≤ 0.06 – 4 µg/mL. These

values were lower than what was found for the comparator imipenem. Of the antibiotics tested

here, only colistin exhibited a similar potency to **1 (-)**. This suggests that our novel LpxC

inhibitor would provide a broad coverage of *P. aeruginosa* clinical isolates.

Table 7. Summary of MIC ranges, MIC_{50} and MIC_{90} of **1 (-)** against 180 *Pseudomonas aeruginosa* strains (MIC in µg/mL).

Compound	Range	MIC_{50}	MIC_{90}
1 (-)	≤ 0.06 – 4	1	2
Amikacin	≤ 0.25 - >1024	16	>128
Tobramycin	≤ 0.125 - >128	2	>128
Azithromycin	≤ 0.25 - >1024	16	>128
Ceftazidime	≤ 0.25 - >128	4	>128
Imipenem	0.06 - > 64	2	16
Piperacillin	0.5 - >128	32	>128
Ticarcillin	0.5 - >128	128	>128
Ciprofloxacin	≤ 0.125 - >64	4	64
Doripenem	≤ 0.03 - >64	1	32
Meropenem	≤ 0.03 - >64	2	32
Colistin	≤ 0.25 - 4	0.5	2

Next, a standard *in vivo* rodent i.v. pharmacokinetics PK study on **1(-)** revealed good blood/plasma exposure and half-life, and this information was used to select the doses and routes of administration for assessment of *in vivo* efficacy. The efficacy of **1 (-)** was evaluated in the neutropenic mouse model of pneumonia, infecting with a clinical isolate of *P. aeruginosa* (MIC = 1 µg/mL) and results are summarized in Figure 5. Mice were dosed twice a day (BID) with **1 (-)**, 2 and 8 hours post infection, and the bacterial burden of the lungs was evaluated at 24 hours post infection. Bacterial stasis (static dose) was achieved at 7.1 mg/kg/day with **1 (-)** and 20 mg/kg/day gave reductions in bacterial burden of the the infected mice of approximately 2-log below stasis. At 20 mg/kg/day both **1 (-)** and ciprofloxacin gave similar reductions in bacterial lung burden at 25 hours post infection compared to noninfected animals.

Figure 5. *P.a.* mouse lung efficacy, BID dosing.
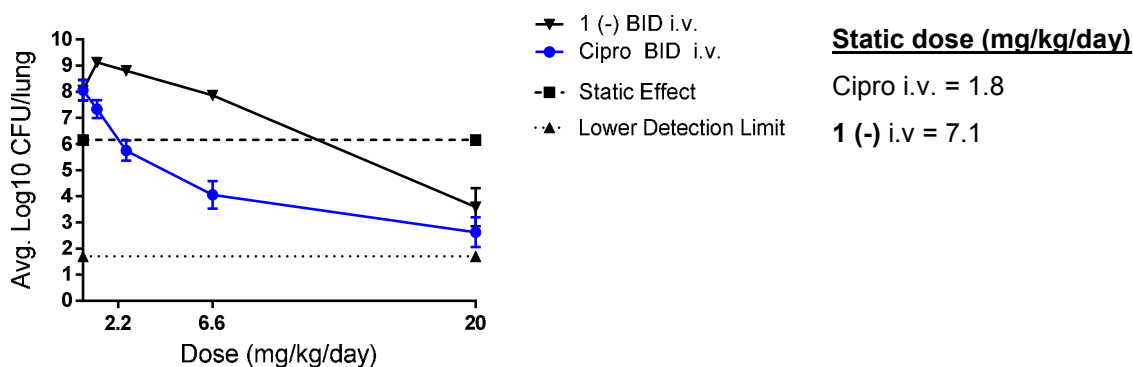
Efficacy against *P. aeruginosa* in the mouse thigh model is shown in Figure 6. The bacterial load (cfu/thigh) at the start of therapy was 4.99 $\log_{10}$ and increased to 8.95 $\log_{10}$ 24 hours later in vehicle treated mice. Treatment with **1(-)** at a single dose of 320 and 160 mg/kg was sufficient to significantly reduce the bacterial burden in thighs from vehicle treated animals to levels before those at the start of treatment.

Figure 6. Efficacy of **1 (-)** against *P. aeruginosa* in the mouse thigh infection model. Neutropenic mice were infected with *P. aeruginosa* and treated subcutaneously 2 hours later with **1 (-)** or vehicle * $P<0.05$, *** $P<0.001$ versus vehicle, Kruskal-Wallis ANOVA followed by a Dunn's multiple comparison test.
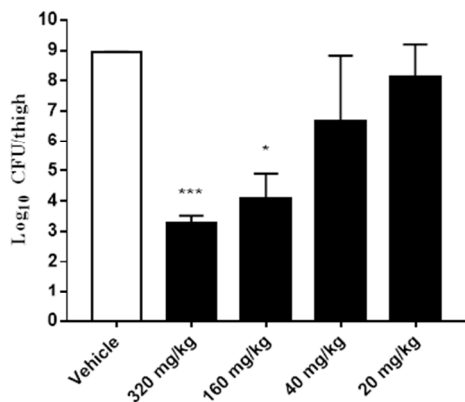
DISCUSSION AND CONCLUSIONS

Here we describe the design of small molecule hydroxamate inhibitors of LpxC as potential new antibacterial agents for the treatment of serious *P. aeruginosa* infections. Hydroxamate **2** was employed as a starting point for a comprehensive structure based medicinal chemistry effort to established detailed SAR relationships, allowing for the elimination of cytotoxicity of compound **2** and retention of potent anti-pseudomonal activity, exemplified by compound **1(-)**. The antibacterial spectrum of **1(-)** is largely confined to *P. aeruginosa*, however it has potent and broad activity across a range of *P. aeruginosa* clinical isolates including those that are resistant to currently used antibiotics. The specificity of compound **1**(-) for *P. aeruginosa* is consistent with several reports highlighting structural variation in the conformation/flexibility of

the substrate-binding tunnel of the LpxC enzyme among Gram-negative bacteria that can in part

modulate susceptibility to LpxC inhibitors[12, 21, 38-40]. Recently, inhibitors having a diacetylene

moiety in the tail region were shown to overcome some of this intrinsic target variability[21]. We

hypothesize that the lack of a diacetylene in **1**(-), along with its relatively small propargyl ether

substitution that is both less bulky and non-linear favors specific inhibition of *P. aeruginosa*

LpxC. There is, however, measureable antibacterial activity of compound **1**(-) against other

Gram-negatives (Table 7), and the MIC can vary among different strains or mutants, reaching

values as low as 1-2 μg/mL against efflux deficient or membrane permeable mutants of *E. coli*

(data not shown). These data suggest that the LpxC target is being inhibited in some Gram-

negative bacteria other than *P. aeruginosa*, but there may be insufficient cellular accumulation of

the compound in wild type cells to mediate potent antibacterial activity. Indeed, the

physicochemical properties of novel inhibitors such as logD may differentially impact whole cell

activity against different Gram-negative pathogens as was recently reported for a series of novel

topisomerase inhibitors[41]. This, combined with the potential differences in susceptibility of the

targets to inhibition by compound **1**(-) described above, likely determines the clinically useful

spectrum of compound **1**(-) antibacterial activity. Nonetheless, our data here show that inhibitors

such as **1(-)** can be designed that may be expected to have good clinical coverage of the highly

adaptable and particularly recalcitrant pathogen *P. aeruginosa*. Interest in more pathogen-

specific antibacterials has been increasing, proportional to the apparent difficulties in finding

broad-spectrum antibiotics, and given the notion that a broad spectrum may contribute to

antibacterial cross-resistance and also unintentionally disturb the human microbiome. Consistent

with the potent *in vitro* activity of **1(-)**, acceptable efficacy was observed in the neutropenic

mouse pneumonia and thigh models of infection using i.v. administration. These results would

1
2
3
4
5
6
7
8
9
10
11
12
13
14
15
16
17
18
19
20
21
22
23
24
25
26
27
28
29
30
31
32
33
34
35
36
37
38
39
40
41
42
43
44
45
46
47
48
49
50
51
52
53
54
55
56
57
58
59
60

warrant further *in vivo* investigations to fully understand PK/PD parameters and subsequent human dose predictions. As well, the translation of the excellent *in vitro* antibacterial activity of **1(-)**, to animal models of infection shown here further supports LpxC as an attractive target against which new inhibitors with *in vivo* efficacy can be designed.

EXPERIMENTAL SECTION

Compound synthesis and characterization.

Compound purity was assessed by HPLC and all tested compounds were > 95% except compound **6** (Table 2), which was 93%. All solvents employed were commercially available anhydrous grade, and reagents were used as received unless otherwise noted. Flash column chromatography was performed on either an Analogix Intelliflash 280 using Si 50 columns (32-63 μm, 230-400 mesh, 60Å) or on a Biotage SP1 system (32-63 μm particle size, KP-Sil, 60 Å pore size).

NMR: proton spectra are recorded on a Bruker 400 MHz ultrashield spectrometer. Chemical shifts are reported relative to dimethyl sulfoxide (δ 2.50) or tetramethylsilane (δ 0.0). Chemical shifts (δ) are reported in parts per million (ppm), and signals are reported as s (singlet), d (doublet), t (triplet), q (quartet), m (multiplet), or br s (broad singlet).

LC/MS: Analytical LC-MS was conducted using an Agilent 1100 series with UV detection at 214 nm and 254 nm, and an electrospray mode (ESI) coupled with a Waters ZQ single quad mass detector.

HPLC: Preparative high pressure liquid chromatography was performed using a Waters 2525 pump with 2487 dual wavelength detector and 2767 sample manager. purification utilizes a C8 or C18 column (30 x 100mm, 5 μm, brand: Sunfire or XTerra) and is performed with 3% n-propanol in 5%-95% ACN in H_2O.

Synthesis of compound 20.

  (S,E)-2-Methyl-N-(2,2,2-trifluoroethylidene)propane-2-sulfinamide (16). Synthesis of sulfinamide **16** was performed according to previously described procedures[42].

  Ethyl(2S,3R)-3-(((S)-tert-butyl(hydroxy)-l4-sulfanyl)amino)-2-((diphenylmethylene)-amino)-4,4,4-trifluorobutanoate (17). To a solution of N-(diphenylmethyleneglycine) ethyl

ester (11.68 g, 43.68 mmol) in anhydrous THF (400 mL) at -78 $^\circ$C was added 1N LiHMDS in

THF (43.68 mL, 43.68 mmol) dropwise. The solution was stirred for 1 h and then the reaction

mixture of **16** in toluene (27.3 mmol, 53 mL) was added slowly. The reaction mixture was

stirred at -78 $^\circ$C for 30 minutes, then quenched by addition of sat. aq. NH_4Cl (150 mL), and

warmed to room temperature. The aqueous phase was extracted with EtOAc. The combined

organic phases were washed with brine, dried over anhydrous Na_2SO_4, and concentrated in

vacuo. The residue was chromatographed on silica gel (gradient: 10% to 40% EtOAc/heptane)

to afford compound **17** (2.15 g) as the major isomer. Found m/z ES^+ = 468. Assignment of its

absolute stereochemistry is based on similar previously described reactions[43].

Ethyl (2S,3R)-2,3-diamino-4,4,4-trifluorobutanoate (18). To a solution of compound **17**

(200 mg, 0.427 mmol) in anhydrous ethanol (1.15 mL) was added 4N HCl in 1,4-dioxane (0.32

mL, 1.28 mmol). The reaction mixture was stirred at room temperature for 1 h. The volatiles

were evaporated under reduced pressure. To the residue was added in sequence THF (2 mL) and

aq. 2M HCl (0.43 mL). The reaction was stirred at room temperature for 2 hrs. The reaction

mixture was then diluted with aq. 1M HCl (15 mL). The aqueous phase was washed with diethyl

ether. The aqueous layer was freeze dried to afford **18** (90 mg; ES^+ *m/z* = 146).

4-(But-2-yn-1-yloxy)benzoyl chloride (intermediate A) was prepared by refluxing the

carboxylic acid **26 (**2.0 g, 10.53 mmol; the synthesis of compound **26** can be found in supporting

information), thionyl chloride (10.2 mL) and catalytic amount of DMF in dichloromethane (50

mL) overnight. The volatiles are removed under reduced pressure to afford intermediate **A** which

was used directly in the next step in preparing compound **19**.

Ethyl (2S,3R)-3-amino-2-(4-(but-2-yn-1-yloxy)benzamido)-4,4,4-trifluorobutanoate (19).

A mixture of **18** (40 mg, 0.147 mmol) in 1,4-dioxane (1.1 mL), intermediate **A** (30.65 mg, 0.147

mmol)*,* NaHCO$_3$ (49.4 mg, 0.588 mmol) and water (1.1 mL) was stirred at room temperature for 36 hs. Then the reaction mixture was diluted with water and extracted with dichloromethane. The organic layer was dried over anhydrous Na$_2$SO$_4$, filtered and concentrated in vacuo. The crude residue was then purified with HPLC (3% n-propanol/Acetonitrile/H$_2$O) to give compound **19** (18 mg). Found ES$^+$ *m/z* = 373.

N-((2S,3R)-3-Amino-4,4,4-trifluoro-1-(hydroxyamino)-1-oxobutan-2-yl)-4-(but-2-yn-1-yloxy)benzamide (20). To a solution of **19** (18 mg, 0.05 mmol) in 2:1 acetontrile/methanol (2.25 mL) was added 50% aq. hydroxylamine (2 mL) and the reaction mixture was stirred at room temperature overnight. The reaction mixture was then purified with preparative HPLC to give compound **20** (5 mg). Found ES$^+$ *m/z* = 360 [M+H]$^+$. ^{1}H NMR (400 MHz, MeOD) δ 7.84 (d, 2H), 7.03 (d, 2H), 5.00 (d, 1H), 4.73 (s, 2H), 3.91 (m, 1H), 1.81 (s, 3H).

Synthesis of compound 30.

(2S,3R)-Methyl 3-hydroxy-2-(tritylamino)butanoate (23). To a solution of L-threonine methyl ester (3.85 g, 22.7 mmol) in anhydrous DCM (30 mL) was added anhydrous TEA at 0 ^{o}C. Then a solution of Trityl chloride (6.59 g, 23.15 mmol) in DCM (30 mL) was added dropwise in 5 min. The reaction mixture was stirred at room temperature overnight. The solid was filtered out and the filtrate was washed with aq. sat. NaHCO$_3$ solution and the aq. layer was extracted with DCM twice. All organic layers were combined, dried over Na$_2$SO$_4$ and filtered. Volatiles were removed under reduced pressure to afford quantitive yield of the title compound. ^{1}H NMR (400 MHz, Chloroform-*d*) δ 7.54 – 7.46 (m, 6H), 7.31 (dtd, *J* = 8.3, 4.4, 3.6, 2.6 Hz, 6H), 7.24 (qt, *J* = 6.1, 0.9 Hz, 3H), 3.86 (td, *J* = 8.1, 7.0, 5.2 Hz, 1H), 3.43 (d, *J* = 7.5 Hz, 1H), 3.19 (s, 3H), 1.23 (d, *J* = 6.2 Hz, 3H).

(2S,3S)-Methyl 3-azido-2-(tritylamino)butanoate (24). To a mixture of (2S,3R)-methyl 3-hydroxy-2-(tritylamino)butanoate (2.35 g, 6.26 mmol) and PPh$_3$ (2.46 g, 9.39 mmol) in THF(30 mL) was added a solution of DIAD (2.03, 9.51 mmol) in THF (15 mL) dropwise at 0 ^{O}C. Then a solution of DPPA (2.84 g, 10.01 mmol) in THF (20 mL) was added dropwise over 5 min. Then the reaction mixture was stirred at rt overnight. Volatiles are removed under reduced pressure and the residue was purified with silica-gel chromatography (10-15% EtOAc/heptane) and another silica-gel chromatography (30% DCM/heptane) to afford the title compound (1.59 g, 63%). ^{1}H NMR (400 MHz, Chloroform-*d*) δ 7.59 – 7.50 (m, 6H), 7.40 – 7.26 (m, 6H), 7.26 – 7.18 (m, 3H), 3.92 – 3.80 (m, 1H), 3.50 (d, *J* = 7.0 Hz, 1H), 3.23 (s, 3H), 3.02 (d, *J* = 19.4 Hz, 1H), 1.26 (d, *J* = 6.9 Hz, 3H).

Methyl (2S,3S)-2-azido-3-azidobutanoate (25). To a solution of (2S,3S)-methyl 3-azido-2-(tritylamino)butanoate (1.1 g, 2.74 mmol) in THF (20 mL) was added a HCl solution (2M in Et$_2$O, 13.7 mL, 27.4 mmol) at 0 ^{O}C. Then the reaction mixture was stirred at rt overnight. Volatiles were removed under reduced pressure and to the residue was added anhydrous Et$_2$O. White solid can be seen formed on the bottom of the flask. Rinse with anhydrous Et$_2$O twice and keep the white solid which was then dried under vacuum to afford crude HCl salt of the title compound (0.50 g) which was used directly in the next step without further purification. ^{1}H NMR (400 MHz, DMSO-*d*$_6$) δ 8.80 (s, 4H), 4.25 (d, *J* = 3.6 Hz, 2H), 3.78 (s, 3H), 1.39 (d, *J* = 6.6 Hz, 3H).

(2S,3S)-methyl 3-azido-2-(4-(but-2-ynyloxy)benzamido)butanoate (27). A mixture of HCl salt of methyl (2S,3S)-2-azido-3-azidobutanoate (307 mg, 1.58 mmol) from previous step, 4-(but-2-ynyloxy)benzoic acid (**26**) (455mg, 2.39 mmol; its synthesis can be found in supporting information), HATU (955 mg, 2.51 mmol), DIPEA (928 mg, 7.18 mmol) in DCM (10 mL) was

stirred at rt for 4 h. Volatiles were removed under reduced pressure and the residue was purified with silica-gel chromatography (10-20% EtOAc/Heptane) three times to afford the title compound (403 mg, 51%). ES$^+$ m/z = 331.1 [M+H]$^+$; ^{1}H NMR (400 MHz, Chloroform-d) δ 7.84 – 7.77 (m, 2H), 7.09 – 7.00 (m, 2H), 6.88 (d, J = 7.7 Hz, 1H), 4.90 (dd, J = 7.8, 3.6 Hz, 1H), 4.73 (q, J = 2.3 Hz, 2H), 4.04 (qd, J = 6.9, 3.7 Hz, 1H), 3.86 (s, 3H), 1.89 (t, J = 2.3 Hz, 3H), 1.48 (d, J = 6.9 Hz, 3H).

(2S,3S)-methyl2-(4-(but-2-ynyloxy)benzamido)-3-(tert-butoxycarbonylamino)butanoate

(28). To a solution of (2S,3S)-methyl 3-azido-2-(4-(but-2-ynyloxy)benzamido)butanoate (400 mg, 1.21 mmol) in MeOH (5 mL) was added SnCl$_2$ (2.30 g, 12.11 mmol). The reaction mixture was stirred at rt for 3 h. Volatiles were removed under reduced pressure. Then to the residue was added DCM (10 mL) and aq. sat. NaHCO$_3$ (20 mL) followed by Boc$_2$O (794, 3.64 mmol). The reaction mixture was stirred at rt for 2 h followed by extracting with DCM (5x). All DCM layers were combined and dried over anhydrous Na$_2$SO$_4$. The solid was filtered out and the filtrate was concentrated followed by purification with silica-gel chromatography (10-25% EtOAc/heptane) to afford white solid as the title compound (409 mg, 83%). ES$^+$ m/z = 405.2 [M+H]$^+$; ^{1}H NMR (400 MHz, Chloroform-d) δ 7.84 (d, J = 8.8 Hz, 2H), 7.64 (d, J = 5.8 Hz, 1H), 7.08 – 6.97 (m, 2H), 5.10 (d, J = 7.8 Hz, 1H), 4.77 (d, J = 4.4 Hz, 1H), 4.72 (q, J = 2.3 Hz, 2H), 4.23 (m, 1H), 3.81 (s, 3H), 1.89 (t, J = 2.3 Hz, 3H), 1.49 (s, 9H), 1.29 (d, J = 6.9 Hz, 3H).

(2S,3S)-methyl 3-amino-2-(4-(but-2-ynyloxy)benzamido)butanoate (29). To a solution of (2S,3S)-methyl 2-(4-(but-2-ynyloxy)benzamido)-3-(tert-butoxycarbonylamino)butanoate (480 mg, 1.19 mmol) in DCM (10 mL) was added TFA (1.83 mL, 2.71 g, 23.74 mmol). The reaction mixture was stirred at rt for 1 h. Volatiles were removed under reduced pressure to afford the

residue as the TFA salt of the title compound which was used directly in the next step. ES$^+$ *m/z* = 305.2 [M+H]$^+$.

N-((2S,3S)-3-amino-1-(hydroxyamino)-1-oxobutan-2-yl)-4-(but-2-ynyloxy)benzamide

(30). To the residue obtained from previous step was added MeOH (3 mL) and NH$_2$OH (aq. 50%, 2 mL) and the solution was stirred at rt overnight. White solid can be seen precipitated out. The solid was filtered, rinsed with water multiple times, then with MeOH, dried under vacuum to afford the title compound (297 mg, 82%). HRMS: C$_{15}$H$_{19}$N$_3$O$_4$ [M+H]$^+$, calc. 306.1448, found 306.1454; ^{1}H NMR (400 MHz, DMSO-d_6) δ 8.14 (d, J = 8.0 Hz, 1H), 7.86 (d, J = 8.8 Hz, 2H), 7.01 (d, J = 8.8 Hz, 2H), 4.80 (q, J = 2.3 Hz, 2H), 4.60 (bs, 2H), 4.16 (t, J = 7.5 Hz, 1H), 3.13 (q, J = 6.8 Hz, 1H), 1.83 (t, J = 2.3 Hz, 3H), 1.02 (d, J = 6.5 Hz, 3H).

The synthesis of other compounds described in this manuscript can be found in supporting information.

Determination of inhibition of LpxC activity (IC$_{50}$ determination)

The assay was carried out using the LC-MS/MS method as described previously [44]. The LpxC substrate, UDP-3-O-R-3-hydroxydecanoyl)-N-acetylglucosamine, was synthesized by the Alberta Research Council (Alberta, Canada). Briefly, assays were performed in a 96-well plate containing PaLpxC (1nM) and LpxC inhibitor (various concentrations initially pre-incubated for 30 minutes at room temperature prior to the addition of substrate at 2µM). Reactions were conducted for 20 minutes at room temperature before being quenched with the stop solution (20% acetic acid). Product formation was quantified using the LC-MS/MS method. The IC$_{50}$ (concentration of inhibitor resulting in half maximal enzyme activity) was determined in XLFit by fitting the data with the following equations and using curve fit dose response model 205:

Equation for calculation of percent inhibition

$$\%\text{Inhibition} = [1 - \frac{(\text{peak area inhibited sample} - \text{peak area of 0\% activity control})}{(\text{peak area uninhibited control} - \text{peak area of 0\% activity control})}] \times 100$$

Four-parameter logistic equation (XLfit equation 205)

$$\text{Percent inhibition} = [\frac{(B - A)}{1 + (\frac{[I]}{IC_{50}})^{D}}] + A$$

where, [I] is the inhibitor concentration and D is the Hill Slope.

A = Response at infinite dose

B = Response at zero dose

I = inhibitor concentration

D = Hill Slope

Bacterial strains and growth conditions

Bacterial strains were from the Novartis Culture Collection, originating as clinical isolates obtained from various geographical areas in the USA, Canada, and Europe. Additional strains were also purchased from American Type Culture Collection (ATCC). The bacterial strains were grown in cation adjusted Mueller Hinton broth. Amikacin and colistin were purchased from Sigma Chemical Co. Tobramycin, aztreonam, ceftazidime, imipenem, piperacillin,

ticarcillin, ciprofloxacin, and meropenem were purchased from USP. Doripenem was purchased from Ortho-McNeil Pharmaceuticals as "Doribax". The LpxC inhibitor, **1 (-)** was synthesized at Novartis. Test compounds were dissolved in DMSO prior to preparation of serial dilutions, with the exception of imipenem, doripenem, and meropenem, which were solubilized in water.

Preparation of antibiotics for drug dilutions

Stock solutions of **1 (-)** and control antibiotics were prepared at 12.8 mg/ml in DMSO, unless noted otherwise. All drug weights were corrected for salt forms and refer to the pure drug substance. Compounds were serially diluted in DMSO, and the carbapenems were serially diluted in water, prior to their introduction into the microtiter test plates.

Antibacterial susceptibility testing

Antibacterial assays to determine Minimum Inhibitory Concentrations (MIC) were performed according to Clinical and Laboratory Standards Institute (CLSI) guidelines [45]. The MIC of the compound was defined as the lowest concentration of drug that prevented visual growth after incubation at 37° C for 18 to 24 hours. MIC_{50} and MIC_{90} values were the minimal drug concentrations required to inhibit 50% or 90% of tested isolates respectively.

Cytotoxicity testing in mammalian cell lines

Dose dependent effects of test compounds on K562 and HepG2 (ATCC) cell metabolic activity were determined for cells exposed to compounds for 72 hours, using cleavage of WST-1 (Roche, Mannheim, Germany). WST-1 is a tetrazolium salt reagent which is reduced and cleaved to formazan by NAD-dependent dehydrogenases and production of formazan was monitored spectrophotometrically (A_{450}). Cells were grown and assayed in medium containing 10% heat

inactivated fetal bovine serum (FBS). The highly cytotoxic, non-selective protein synthesis inhibitor puromycin [46] was used as a positive control. Values for cytotoxicity (CC_{50}) were calculated from the dose response curves and represent the concentration required to cause a 50 % reduction in cell viability.

Crystallography

A *P.a* LpxC construct encoding amino acids 1-299 (PaLpxC 1-299) was expressed in BL21 (DE3) pLysS cells (Promega) at 28 °C for 2.5 hours post IPTG-induction. Cells were harvested by centrifugation, resuspended in 50 mM Hepes pH 7.0, 0.5 mM ZnCl2, 1 mM TCEP, 5 mM MgCl2, 50 ug/ml DNase I, EDTA-free cOmplete Protease Inhibitor Tablets (Roche) and lysed with a Microfluidizer (Microfluidics). The conductivity of the clarified lysate was adjusted to < 2.5 mS/cm using 50 mM Hepes pH 7.0, 1 mM TCEP followed by purification on Q Sepharose FF resin (GE Healthcare) using an elution buffer containing 50 mM HEPES pH 7.0, 100 mM NaCl, 1 mM TCEP. Fractions containing PaLpxC 1-299 were pooled and mixed with solid NaCl, resulting in a final concentration of 4 M NaCl, loaded onto a Butyl HP HiTrap column (GE Healthcare) and eluted with a gradient from 3.6 M to 0 M NaCl. Fractions were then buffer exchanged into 20 mM Tris pH 7.0, 1 mM TCEP for further purification on a MonoQ column (GE Healthcare) using an elution gradient from 0 to 500 mM NaCl. The PaLpxC 1-299 pool was reloaded with Zn^{2+} by buffer exchange into 25 mM HEPES pH 7, 500 mM NaCl, 1 mM TCEP, 0.1 mM $ZnCl_2$ (2-fold molar excess Zn^{2+}), concentrated and loaded onto a HiLoad Superdex 75 16/60 column (GE Healthcare) equilibrated in 25 mM HEPES pH 7, 150 mM NaCl, 1 mM TCEP. Purified PaLpxC 1-299 was concentrated to 10 mg/ml, frozen in liquid nitrogen and stored at -80 °C.

PaLpxC 1-299 was incubated with **1(-)** at a molar ratio of 1:1.5 and screened for crystallization at 20 °C. Initial crystals grew from drops containing equal volume of protein and reservoir solution containing 0.1 M HEPES pH 7.0, 0.2 M $MgCl_2$ and 10-20 % PEG 3350. Crystals used for data collection were grown in drops that were streak-seeded with nuclei from drops containing small crystals. Crystals were transferred to cryo-protection solution containing an additional 25% glycerol and flash cooled in liquid nitrogen. Data were collected at 100K using a Pilatus 6M detector and synchrotron radiation (λ=0.99980Å) at the Swiss Light Source beam line X06SA and processed with the XDS software package [47]. The structure was solved by molecular replacement with Phaser [48] in the spacegroup $P2_12_12_1$ (a=35.8, b=98.4, c=165.2, α=β=γ=90°) using a previously determined in-house PaLpxC 1-299/inhibitor complex structure as a starting model. Iterative cycles of building using COOT[49] and refinement using initially PHENIX[50] and then BUSTER (Global Phasing, Ltd) led to a final model with R_{free}=21.3% (5% test set) and R_{work}=18.6% using all of the data from 82.6-2.0 Å. The structure factors and coordinates have been deposited in the RCSB PDB with accession code 5U3B.

Molecular Docking

Docking studies of LpxC inhibitors were performed using Glide (Schrödinger, LLC) with the Single Precision (SP) scoring function. The ligands in the docking study were prepared using LigPrep (Schrödinger, LLC). The binding region was defined by a 30 Å × 30 Å × 30 Å grid box centered on the binding site of the *Pseudomonas aeruginosa* LpxC (PaLpxC/**31** structure, PDB code: 5U39). Default settings were used for all the parameters.

Animal infection models. All animal experiments were approved by and conducted in accordance with the guidelines of the Intuitional Animal Care and Use Committee of Novartis. Animals were maintained under controlled conditions with free access to food and water.

Pneumonia infection model. Mice (n=5, female BalbC, 18 to 20 g Charles River Laboratories, Wilmington, MA) were rendered neutropenic by intraperitoneal injections of cyclophosphamide (Sigma Chemical Co., St. Louis, Mo.), on days -4 and -1 respectively prior to infection. Animals were then infected intranasally two hours prior to treatment (-2 h), with *P. aeruginosa* at approximately $1x10^5$ CFU/mouse. At time 0 hours (0 h), animals were treated with **21 (-)** or ciprofloxacin via the i.v. route of administration (BID at 2 and 6 hours post infection). At 24 hours post infection mice were sacrificed and the lungs removed for bacterial enumeration. Data were expressed as $\log_{10}$ cfu/lung and presented as mean ± SD for each dosing group. The static dose (mg/kg/day) is the dose of drug which maintains the level of bacteria at the start of treatment (0H). Dose/day was plotted against $\log_{10}$ cfu and analyzed using a four parametric logistic curve (SigmaPlot 12.0, SyStat Software, San Jose, California). The static dose was calculated using the following equation: $\log_{10}$ static dose $=\{\log_{10}[E/(E_{max} - E)]/N \} + \log10$ ED_{50}, where, E is the control growth ($\log_{10}$ change in cfu per thigh in untreated controls after the 24-h period of study), E_{max} is the maximum effect, ED_{50} is the dose required to achieve 50% of E_{max}, and N is the slope of the dose effect curve.

Thigh infection model. Mice were rendered neutropenic by 2 injections of cyclophosphamide (Sigma Chemical Co., St. Louis, Mo.) at doses of 150 mg/kg intraperitoneally (i.p.) and 100 mg/kg i.p. 4 and 1 day prior to infection respectively. Thigh infections were established by intramuscular injection of 50μl of a freshly prepared bacterial suspension of ATCC 27853 (approx 6×10^5 cfu/thigh) into the left hind thigh of female CD1mice (n=4, 20 to 25 g

Charles River Laboratories, Wilmington, MA). **1 (-)** was formulated in PBS and administered subcutaneously 2 hours post infection at doses of 320, 160, 40 and 20 mg/kg. Control mice were treated with vehicle only. Twenty four hours after start of treatment, the mice were euthanized and the thighs aseptically excised. Thigh muscles were homogenized in 5 ml saline, and appropriate dilutions were plated onto blood agar plates to determine the number of viable bacteria per thigh. The detection limit was 100 CFU/thigh. Differences in the mean values of the bacterial count per thigh between antibiotic treated mice and control were analyzed by the Kruskal-Wallis ANOVA followed by a Dunn's multiple comparison test (GraphPad Prism 7.0).

ASSOCIATED CONTENT

Supporting information

Details of compound syntheses not described in main text experimental section **(PDF)**

Molecular formula strings (**CSV**)

PDB ID codes

The structure factors and coordinates for PaLpxC complexed with **1(-)** and **31** have been

deposited in the RCSB PDB with accession codes 5U3B and 5U39, respectively. Authors will

release the atomic coordinates and experimental data upon article publication.

AUTHOR INFORMATION

Corresponding authors

*C.R.D.; E-mail, charlesr.dean@novartis.com; Phone: 510-879-9564
*G.P.; E-mail, grazia.pzz@gmail.com; Phone: 207-319-3898

Current affiliations :

G.P., Merck Exploratory Science Center (ESC), Cambridge, MA, USA

J.B, NGM Biopharmaceuticals, Boston, MA, USA

L.G.H., Celgene corporation, Cambridge, MA, USA

M.G., Merck Research Laboratories, Boston, MA, USA

R.T., Entasis Therapeutics, Waltham, MA, USA

X.Y., Shire Pharmaceuticals, Lexington, MA

ORCID

Charles Dean: 0000-0001-9858-9818

Abbreviations used

ACN, acetonitrile; aq, aqueous; Boc_2O, di-tert-butyl dicarbonate; DIAD, diisopropyl azodicarboxylate; DPPA, diphenoxyphosphoryl azide; DIPEA, N-Ethyldiisopropylamine; DCM, dichloromethane; DMF, dimethylformamide; DMSO, dimethylsulfoxide; Et_2O, diethylether; EtOAc, ethyl acetate; g, gram; HATU, 1-[bis(dimethylamino)methylene]-1H-1,2,3-triazolo[4,5-b]pyridinium 3-oxid hexafluorophosphate); HCl, hydrochloric acid; h, hour(s); HRMS,high resolution mass spectrum; HPLC, high pressure liquid chromatography; LC, liquid chromatography; LC/MS, liquid chromatography mass spectrum; LiHMDS, lithium bis(trimethylsilyl)amide; mg, milligram; mL, milliliter; MeOH, methanol; Min, minute(s); MHz, megahertz, 10^6 Hz; MIC, minimal inhibitory concentration; NH_4Cl, ammonium chloride; NH_2OH, hydroxylamine; $NaHCO_3$, sodium bicarbonate; Na_2SO_4, sodium sulfate; PPh_3, triphenyl phosphine; rt, room temperature; SI, supplemental information; $SnCl_2$, Tin(II) chloride; TFA, trifluoroacetic acid; TEA, triethylamine; sat, saturated; *m/z*, mass to charge ratio; THF, tetrahydrofuran.

REFERENCES

(1)   Rossolini, G. M.; Arena, F.; Pecile, P.; Pollini, S. Update on the antibiotic resistance crisis. *Curr. Opin. Pharmacol.* **2014,** *18*, 56-60.

(2)   Nikaido, H. Molecular basis of bacterial outer membrane permeability revisited. *Microbiol. Mol. Biol. Rev.* **2003,** *67*, 593-656.

(3)   Raetz, C. R.; Whitfield, C. Lipopolysaccharide endotoxins. *Annu. Rev. Biochem.* **2002,** *71*, 635-700.

(4)   Li, X. Z.; Plesiat, P.; Nikaido, H. The challenge of efflux-mediated antibiotic resistance in Gram-negative bacteria. *Clin. Microbiol. Rev.* **2015,** *28*, 337-418.

(5)   Poole, K. Outer membranes and efflux: the path to multidrug resistance in Gram-negative bacteria. *Curr. Pharm. Biotechnol.* **2002,** *3*, 77-98.

(6)   Moffatt, J. H.; Harper, M.; Harrison, P.; Hale, J. D.; Vinogradov, E.; Seemann, T.; Henry, R.; Crane, B.; St Michael, F.; Cox, A. D.; Adler, B.; Nation, R. L.; Li, J.; Boyce, J. D. Colistin resistance in *Acinetobacter baumannii* is mediated by complete loss of lipopolysaccharide production. *Antimicrob. Agents Chemother.* **2010,** *54*, 4971-4977.

(7)   Lin, L.; Tan, B.; Pantapalangkoor, P.; Ho, T.; Baquir, B.; Tomaras, A.; Montgomery, J. I.; Reilly, U.; Barbacci, E. G.; Hujer, K.; Bonomo, R. A.; Fernandez, L.; Hancock, R. E.; Adams, M. D.; French, S. W.; Buslon, V. S.; Spellberg, B. Inhibition of LpxC protects mice from resistant *Acinetobacter baumannii* by modulating inflammation and enhancing phagocytosis. *MBio* **2012,** *3(5)*. pii: e00312-12. doi: 10.1128/mBio.00312-12.

(8)   Garcia-Quintanilla, M.; Caro-Vega, J. M.; Pulido, M. R.; Moreno-Martinez, P.; Pachon, J.; McConnell, M. J. Inhibition of LpxC Increases Antibiotic Susceptibility in *Acinetobacter baumannii*. *Antimicrob. Agents Chemother.* **2016,** *60*, 5076-5079.

(9)   Lee, C. R.; Lee, J. H.; Jeong, B. C.; Lee, S. H. Lipid a biosynthesis of multidrug-resistant pathogens - a novel drug target. *Curr. Pharm. Des*. **2013,** *19*, 6534-6550.

(10)   Onishi, H. R.; Pelak, B. A.; Gerckens, L. S.; Silver, L. L.; Kahan, F. M.; Chen, M. H.; Patchett, A. A.; Galloway, S. M.; Hyland, S. A.; Anderson, M. S.; Raetz, C. R. Antibacterial agents that inhibit lipid A biosynthesis. *Science* **1996,** *274*, 980-982.

(11)   Srinivas, N.; Jetter, P.; Ueberbacher, B. J.; Werneburg, M.; Zerbe, K.; Steinmann, J.; Van der Meijden, B.; Bernardini, F.; Lederer, A.; Dias, R. L.; Misson, P. E.; Henze, H.; Zumbrunn, J.; Gombert, F. O.; Obrecht, D.; Hunziker, P.; Schauer, S.; Ziegler, U.; Kach, A.; Eberl, L.; Riedel, K.; DeMarco, S. J.; Robinson, J. A. Peptidomimetic antibiotics target outer-membrane biogenesis in *Pseudomonas aeruginosa*. *Science* **2010,** *327*, 1010-1013.

(12)   Mdluli, K. E.; Witte, P. R.; Kline, T.; Barb, A. W.; Erwin, A. L.; Mansfield, B. E.; McClerren, A. L.; Pirrung, M. C.; Tumey, L. N.; Warrener, P.; Raetz, C. R.; Stover, C. K. Molecular validation of LpxC as an antibacterial drug target in *Pseudomonas aeruginosa*. *Antimicrob. Agents Chemother.* **2006,** *50*, 2178-2184.

(13)   Murphy-Benenato, K. E.; Olivier, N.; Choy, A.; Ross, P. L.; Miller, M. D.; Thresher, J.; Gao, N.; Hale, M. R. Synthesis, structure, and SAR of tetrahydropyran-based LpxC inhibitors. *A.C.S. Med. Chem. Lett.* **2014,** *5*, 1213-1218.

(14)   Szermerski, M.; Melesina, J.; Wichapong, K.; Loppenberg, M.; Jose, J.; Sippl, W.; Holl, R. Synthesis, biological evaluation and molecular docking studies of benzyloxyacetohydroxamic acids as LpxC inhibitors. *Bioorg. Med. Chem.* **2014,** *22*, 1016-1028.

(150   Hale, M. R.; Hill, P.; Lahiri, S.; Miller, M. D.; Ross, P.; Alm, R.; Gao, N.; Kutschke, A.; Johnstone, M.; Prince, B.; Thresher, J.; Yang, W. Exploring the UDP pocket of LpxC through amino acid analogs. *Bioorg. Med. Chem. Lett.* **2013,** *23*, 2362-2367.

(16)   Montgomery, J. I.; Brown, M. F.; Reilly, U.; Price, L. M.; Abramite, J. A.; Arcari, J.; Barham, R.; Che, Y.; Chen, J. M.; Chung, S. W.; Collantes, E. M.; Desbonnet, C.; Doroski, M.; Doty, J.; Engtrakul, J. J.; Harris, T. M.; Huband, M.; Knafels, J. D.; Leach, K. L.; Liu, S.; Marfat, A.; McAllister, L.; McElroy, E.; Menard, C. A.; Mitton-Fry, M.; Mullins, L.; Noe, M. C.; O'Donnell, J.; Oliver, R.; Penzien, J.; Plummer, M.; Shanmugasundaram, V.; Thoma, C.; Tomaras, A. P.; Uccello, D. P.; Vaz, A.; Wishka, D. G. Pyridone methylsulfone hydroxamate LpxC inhibitors for the treatment of serious Gram-negative infections. *J. Med. Chem.* **2012,** *55*, 1662-1670.

(17)   Brown, M. F.; Reilly, U.; Abramite, J. A.; Arcari, J. T.; Oliver, R.; Barham, R. A.; Che, Y.; Chen, J. M.; Collantes, E. M.; Chung, S. W.; Desbonnet, C.; Doty, J.; Doroski, M.; Engtrakul, J. J.; Harris, T. M.; Huband, M.; Knafels, J. D.; Leach, K. L.; Liu, S.; Marfat, A.; Marra, A.; McElroy, E.; Melnick, M.; Menard, C. A.; Montgomery, J. I.; Mullins, L.; Noe, M. C.; O'Donnell, J.; Penzien, J.; Plummer, M. S.; Price, L. M.; Shanmugasundaram, V.; Thoma, C.; Uccello, D. P.; Warmus, J. S.; Wishka, D. G. Potent inhibitors of LpxC for the treatment of Gram-negative infections. *J. Med. Chem.* **2012,** *55*, 914-923.

(18)   McAllister, L. A.; Montgomery, J. I.; Abramite, J. A.; Reilly, U.; Brown, M. F.; Chen, J. M.; Barham, R. A.; Che, Y.; Chung, S. W.; Menard, C. A.; Mitton-Fry, M.; Mullins, L. M.; Noe, M. C.; O'Donnell, J. P.; Oliver, R. M., 3rd; Penzien, J. B.; Plummer, M.; Price, L. M.; Shanmugasundaram, V.; Tomaras, A. P.; Uccello, D. P. Heterocyclic methylsulfone hydroxamic acid LpxC inhibitors as Gram-negative antibacterial agents. *Bioorg. Med. Chem. Lett.* **2012,** *22*, 6832-6838.

(19)   Mansoor, U. F.; Vitharana, D.; Reddy, P. A.; Daubaras, D. L.; McNicholas, P.; Orth, P.; Black, T.; Siddiqui, M. A. Design and synthesis of potent Gram-negative specific LpxC inhibitors. *Bioorg. Med. Chem. Lett.* **2011,** *21*, 1155-1161.

(20)   Titecat, M.; Liang, X.; Lee, C. J.; Charlet, A.; Hocquet, D.; Lambert, T.; Pages, J. M.; Courcol, R.; Sebbane, F.; Toone, E. J.; Zhou, P.; Lemaitre, N. High susceptibility of MDR and XDR Gram-negative pathogens to biphenyl-diacetylene-based difluoromethyl-allo-threonyl-hydroxamate LpxC inhibitors. *J. Antimicrob. Chemother.* **2016,** *71*, 2874-2882.

(21)   Liang, X.; Lee, C. J.; Chen, X.; Chung, H. S.; Zeng, D.; Raetz, C. R.; Li, Y.; Zhou, P.; Toone, E. J. Syntheses, structures and antibiotic activities of LpxC inhibitors based on the diacetylene scaffold. *Bioorg. Med. Chem.* **2011,** *19*, 852-860.

(22)   Liang, X.; Lee, C. J.; Zhao, J.; Toone, E. J.; Zhou, P. Synthesis, structure, and antibiotic activity of aryl-substituted LpxC inhibitors. *J. Med. Chem.* **2013,** *56*, 6954-6966.

(23)   Pirrung, M. C.; Tumey, L. N.; Raetz, C. R.; Jackman, J. E.; Snehalatha, K.; McClerren, A. L.; Fierke, C. A.; Gantt, S. L.; Rusche, K. M. Inhibition of the antibacterial target UDP-(3-O-acyl)-N-acetylglucosamine deacetylase (LpxC): isoxazoline zinc amidase inhibitors bearing diverse metal binding groups. *J. Med. Chem.* **2002,** *45*, 4359-4370.

(24)   Coggins, B. E.; Li, X.; McClerren, A. L.; Hindsgaul, O.; Raetz, C. R.; Zhou, P. Structure of the LpxC deacetylase with a bound substrate-analog inhibitor. *Nat. Struct. Biol.* **2003,** *10*, 645-651.

(25)   Coggins, B. E.; McClerren, A. L.; Jiang, L.; Li, X.; Rudolph, J.; Hindsgaul, O.; Raetz, C. R.; Zhou, P. Refined solution structure of the LpxC-TU-514 complex and pKa analysis of an active site histidine: insights into the mechanism and inhibitor design. *Biochemistry* **2005,** *44*, 1114-1126.

(26)   Barb, A. W.; Jiang, L.; Raetz, C. R.; Zhou, P. Structure of the deacetylase LpxC bound to the antibiotic CHIR-090: Time-dependent inhibition and specificity in ligand binding. *Proc. Natl. Acad. Sci. USA* **2007,** *104*, 18433-18438.

(27)   Bodewits, K.; Raetz, C. R.; Govan, J. R.; Campopiano, D. J. Antimicrobial activity of CHIR-090, an inhibitor of lipopolysaccharide biosynthesis, against the *Burkholderia cepacia* complex. *Antimicrob. Agents. Chemother.* **2010,** *54*, 3531-3533.

(28)   Kurasaki, H.; Tsuda, K.; Shinoyama, M.; Takaya, N.; Yamaguchi, Y.; Kishii, R.; Iwase, K.; Ando, N.; Nomura, M.; Kohno, Y. LpxC Inhibitors: Design, synthesis, and biological evaluation of oxazolidinones as Gram-negative antibacterial agents. *A.C.S. Med. Chem. Lett.* **2016,** *7*, 623-628.

(29)   Erwin, A. L. Antibacterial drug discovery targeting the lipopolysaccharide biosynthetic enzyme LpxC. *Cold Spring Harb. Perspect. Med.* **2016,** *6*. pii: a025304. doi: 10.1101/cshperspect.a025304.

(30)   Kasar, R. L.; M.S.; Aggen, J.B.; Lu, Q.; Wang, D.; Church, T.; Moser, H.E.; Patten, P.A. Preparation of hydroxamic acid derivatives useful in the treatment of bacterial infections. U.S patent WO2012154204A1**,** Nov 15, 2012.

(31)   Anderson, N. H.; Bowman, J.; Erwin, A.; Harwood, E.; Kline, T.; Mdluli, K.; Ng, S.; Pfister, K. B.; Shawar, R.; Wagman, A.; Yabannavar, A. Antibacterial Agents. International Patent WO/2004/062601, July 29, 2004.

(32)   Barb, A. W.; McClerren, A. L.; Snehelatha, K.; Reynolds, C. M.; Zhou, P.; Raetz, C. R. Inhibition of lipid A biosynthesis as the primary mechanism of CHIR-090 antibiotic activity in *Escherichia coli. Biochemistry* **2007,** *46*, 3793-3802.

(33)   Masuda, N.; Ohya, S. Cross-resistance to meropenem, cephems, and quinolones in *Pseudomonas aeruginosa*. *Antimicrob. Agents Chemother.* **1992,** *36*, 1847-1851.

(34)   Li, X. Z.; Zhang, L.; Srikumar, R.; Poole, K. Beta-lactamase inhibitors are substrates for the multidrug efflux pumps of *Pseudomonas aeruginosa*. *Antimicrob. Agents Chemother.* **1998,** *42*, 399-403.

(35)   Angus, B. L.; Carey, A. M.; Caron, D. A.; Kropinski, A. M.; Hancock, R. E. Outer membrane permeability in *Pseudomonas aeruginosa*: comparison of a wild-type with an antibiotic-supersusceptible mutant. *Antimicrob. Agents Chemother.* **1982,** *21*, 299-309.

(36)   Dobler, M. R.; Lenoir, F.; Parker, D.T.; Peng, Y.; Piizzi, G.; Wattanasin, S. Organic compounds for applications in bacterial infections treatment. International Patent *WO/2010/031750,* March 25, 2010

(37)   Fei, Z. B.; Kong, W. Y.; Wang, H. M.; Peng, J. B. A.; Sun, F.; Yin, Y. Y.; Bajwa, J.; Jiang, X. L. A Scalable synthesis of a hydroxamic acid LpxC inhibitor. *Org. Process. Res. Dev.* **2012,** *16*, 1436-1441.

(38)   Lee, C. J.; Liang, X.; Gopalaswamy, R.; Najeeb, J.; Ark, E. D.; Toone, E. J.; Zhou, P. Structural basis of the promiscuous inhibitor susceptibility of *Escherichia coli* LpxC. *A.C.S. Chem. Biol.* **2014,** *9*, 237-246.

(39)   Kadam, R. U.; Shivange, A. V.; Roy, N. *Escherichia coli* versus *Pseudomonas aeruginosa* deacetylase LpxC inhibitors selectivity: surface and cavity-depth-based analysis. *J. Chem. Inf. Model.* **2007,** *47*, 1215-1224.

(40)   Lee, C. J.; Liang, X.; Chen, X.; Zeng, D.; Joo, S. H.; Chung, H. S.; Barb, A. W.; Swanson, S. M.; Nicholas, R. A.; Li, Y.; Toone, E. J.; Raetz, C. R.; Zhou, P. Species-specific

and inhibitor-dependent conformations of LpxC: implications for antibiotic design. *Chem. Biol.* **2011,** *18*, 38-47.

(41)   Reck, F.; Ehmann, D. E.; Dougherty, T. J.; Newman, J. V.; Hopkins, S.; Stone, G.; Agrawal, N.; Ciaccio, P.; McNulty, J.; Barthlow, H.; O'Donnell, J.; Goteti, K.; Breen, J.; Comita-Prevoir, J.; Cornebise, M.; Cronin, M.; Eyermann, C. J.; Geng, B.; Carr, G. R.; Pandarinathan, L.; Tang, X.; Cottone, A.; Zhao, L.; Bezdenejnih-Snyder, N. Optimization of physicochemical properties and safety profile of novel bacterial topoisomerase type II inhibitors (NBTIs) with activity against *Pseudomonas aeruginosa*. *Bioorg. Med. Chem.* **2014,** *22*, 5392-5409.

(42)   Truong, V. L.; Menard, M. S.; Dion, I. Asymmetric syntheses of 1-aryl-2,2,2-trifluoroethylamines via diastereoselective 1,2-addition of arylmetals to 2-methyl-N-(2,2,2-trifluoroethylidene)propane-2-sulfinamide. *Org. Lett.* **2007,** *9*, 683-685.

(43)   Davis, F. A.; Deng, J. Asymmetric synthesis of syn-(2R,3S)-and anti-(2S,3S)-ethyl diamino-3-phenylpropanoates from N-(benzylidene)-p-toluenesulfinamide and glycine enolates. *Org. Lett.* **2004,** *6*, 2789-2792.

(44)   Langsdorf, E. F.; Malikzay, A.; Lamarr, W. A.; Daubaras, D.; Kravec, C.; Zhang, R.; Hart, R.; Monsma, F.; Black, T.; Ozbal, C. C.; Miesel, L.; Lunn, C. A. Screening for antibacterial inhibitors of the UDP-3-O-(R-3-hydroxymyristoyl)-N-acetylglucosamine deacetylase (LpxC) using a high-throughput mass spectrometry assay. *J. Biomol. Screen.* **2010,** *15*, 52-61.

(45)   CLSI. Methods for dilution antimicrobial susceptibility test for bacteria that grow aerobically (M07-A7), CLSI, Wayne, PA. **2006**.

46.   Darken, M. A. Puromycin inhibition of protein synthesis. *Pharmacol. Rev.* **1964,** *16*, 223-243.

(47)   Kabsch, W. Xds. *Acta Crystallogr. D.* **2010,** *66*, 125-132.

(48)   Mccoy, A. J.; Grosse-Kunstleve, R. W.; Adams, P. D.; Winn, M. D.; Storoni, L. C.;

Read, R. J. Phaser crystallographic software. *J. Appl. Crystallogr.* **2007,** *40*, 658-674.

(49)   Emsley, P.; Cowtan, K. Coot: model-building tools for molecular graphics. *Acta*

Crystallogr. D **2004,** *60*, 2126-2132.

(50)   Adams, P. D.; Grosse-Kunstleve, R. W.; Hung, L. W.; Ioerger, T. R.; McCoy, A. J.;

Moriarty, N. W.; Read, R. J.; Sacchettini, J. C.; Sauter, N. K.; Terwilliger, T. C. PHENIX:

building new software for automated crystallographic structure determination. *Acta. Crystallogr.*

D **2002,** *58*, 1948-1954.

TABLE OF CONTENTS GRAPHIC

1 (-)
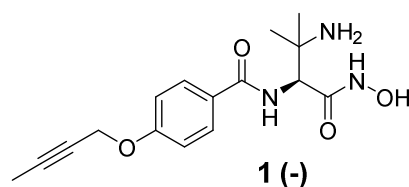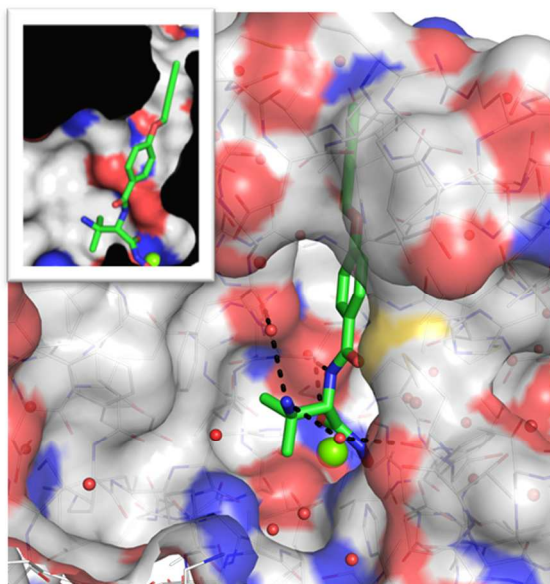
wt *P.a.* LpxC IC_{50} = 1.5 nM
wt *P.a.* MIC = 1.0 μg/mL
MDR *P.a.* MIC_{90} = 2 μg/mL